Heliyon 7 (2021) e06691

Contents lists available at ScienceDirect

Heliyon

journal homepage: www.cell.com/heliyon

Review article

Multi-detector hydrodynamic chromatography of colloids: following in Hamish Small's footsteps

André M. Striegel *

Chemical Sciences Division, National Institute of Standards and Technology (NIST), 100 Bureau Drive, MS 8392, Gaithersburg, MD 20899-8392 USA

ARTICLE INFO

Keywords:
Hamish Small
Hydrodynamic chromatography
Colloids
Multiple detection
Structure property relations

ABSTRACT

Hamish Small, scientist extraordinaire, is best known as the inventor of both ion chromatography and hydrodynamic chromatography (HDC). The latter has experienced a renaissance during the last decade-plus, thanks principally to its coupling to a multiplicity of physicochemical detection methods and to the structural and compositional information this provides. Detection methods such as light scattering (both multi-angle static and dynamic), viscometry, and refractometry can combine to yield insight into macromolecular or colloidal size, structure, shape, and molar mass, all as a function of one another and continuously across a sample's chromatogram. It was the author's great fortune to have known Hamish during the last decade of his life, before his passing in 2019. Here, a brief personal recollection is followed by an introduction to HDC and its application, in quadruple-detector packed-column mode, to the analysis of a commercial colloidal silica with an elongated shape.

1. A personal introduction

On October 21, 2012, I received a very brief e-mail which read, in its entirety:

Dear Dr. Striegel,

I would greatly appreciate receiving copies of your articles on HDC.

thank you

Hamish Small

"HDC" stands for hydrodynamic chromatography and I, of course, knew who Hamish Small was. It took me virtually no time to reply to Hamish (according to my Outlook e-mail records, I did this within 15 min of receiving the reprint request) and to flood him with everything we had published on HDC up to that point [1, 2, 3, 4, 5, 6, 7, 8]. The unintended humor of this was not lost on Hamish, whose reply to me began "Dear Andre, Many thanks for all the articles. That should keep me busy for some time!" This marked the beginning of a correspondence that would carry itself out via e-mail, LinkedIn messages, and snail-mail and would continue until shortly before Hamish's untimely passing in 2019. A particular highlight of these communications was Hamish granting me the honor of interviewing him for *LC-GC Europe* in 2015 [9], an interview which was reprinted soon thereafter in *LC-GC North America* [10]. In this interview, Hamish contrasted performing research in the UK versus in the US, elaborated about performing research while employed at a large chemical company (he spent many years with Dow Chemical), shared his thoughts and advice to a younger generation of scientists, and talked about the development and continued potential of techniques such as ion chromatography (IC) and hydrodynamic chromatography. Most people know Hamish best as the inventor of IC, and rightfully so. One technique, however, for which he may not be as well known in the scientific community at large, but for which he is extremely well-known in the polymer and colloid separations community is HDC. It is the latter that is the topic of this paper.

2. A scientific introduction

Perhaps the simplest way to envisage HDC is to imagine a mobile phase flowing laminarly (*i.e.,* at low Reynold number Re) through an open tube. Within the capillary, a parabolic or Poiseuille-like flow profile will develop, as depicted in Figure 1a in which the arrows are meant to represent the streamlines of flow. Let us further imagine that, into this flow prolife, we inject two particles, a large particle (in orange in Figure 1b) and a small particle (in green in Figure 1b) and that, for the purposes of the present discussion, the position of each particle within the tube can be characterized by that of its center of mass. Because of the larger particle's size, its center of mass will not be able to approach the walls of the tube as closely as will be possible for the center of mass of the smaller particle. Due to this, the larger particle will remain nearer the center of the tube, preferentially experiencing the faster streamlines of

* Corresponding author.
E-mail address: andre.striegel@nist.gov.

https://doi.org/10.1016/j.heliyon.2021.e06691
Received 15 January 2021; Received in revised form 2 March 2021; Accepted 30 March 2021

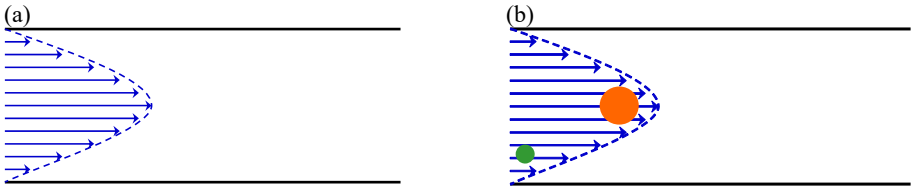

Figure 1. Generic representation of flow profile and analyte separation mechanism in HDC. (a) Parabolic, Poiseuille-like flow profile develops in an open tube of constant cross-section as a result of laminar, low-Re flow; arrows represent streamlines of flow. (b) Larger (orange) analytes remain nearer the center of the tube, preferentially experiencing the faster streamlines, while smaller (green) analytes can approach the tube walls more closely than larger ones, experiencing both fast and slow streamlines and, thus, a slower average velocity as compared to the large analytes.

flow located thereat, while the smaller particle samples both these faster streamlines as well as the slower ones located nearer the walls of the tube. The consequence of this is that the smaller particle travels through the tube with a slower average velocity, and elutes from the tube later, than does its larger counterpart.

The elution order in HDC is the same as in the more common macromolecular separation method size-exclusion chromatography (SEC), as in both methods larger analytes elute ahead of smaller ones. The mechanism of retention differs among the techniques, however. In SEC, retention is due to preferential sampling of pore volume, whereas in HDC retention is due to preferential sampling of streamlines of flow [8, 11].

The first separation by a hydrodynamic-chromatography-type mechanism that appears to have been recognized as such was the work of Kai Pedersen, at the University of Uppsala, in 1962 [12], of which Hamish Small was well-aware and which he referenced in his publications. Pedersen fractionated proteins employing columns packed with impermeable glass beads. For the separation of *Helix* hemocyanin and human serum albumin (HuSA), two wavelengths of absorption were monitored, one at which the hemocyanin absorbed preferentially and the other at which HuSA absorbed. The data for these two absorptions (each ratioed to an appropriate reference wavelength) are represented by the crosses and the open triangles in Figure 2. As can be seen in this figure, each side of the peak shown is enriched in one of the two analytes. Even though the chromatographic resolution for this separation was quite low, by monitoring multiple wavelengths of absorption it could be determined that a separation did, indeed, occur. Pedersen was able to show that separation did not result from adsorption processes, while simultaneously recognizing that the separation took place in the interstitial medium of the column. To explain how this separation happened, Pedersen invoked a tubular pinch flow mechanism in analogy to that by which blood corpuscles travel through the human vascular system. This is now recognized as being too restrictive an explanation for what occurs in HDC in general.

Between 1969 and 1971, Edward DiMarzio and Charles Guttman, at what was then the National Bureau of Standards and is now the National Institute of Standards and Technology (NIST), published a series of theory papers on a technique which they termed "separation by flow" and which we now recognize as being essentially identical to hydrodynamic chromatography in the absence of electrostatic and van der Waals effects [13, 14, 15, 16]. In these publications, DiMarzio and Guttman derived figures of merit for the technique, examined the effects of different capillary cross-sections on the separation, contrasted the separation of colloids to that of polymers, etc. In reference [14] the authors stated that, given the theoretical nature of their work, "The question naturally arises as to whether the separation by flow phenomenon is of any practical use…[T]his can be answered only by construction of a working instrument based on the phenomenon."

It was not long before the question posited by DiMarzio and Guttman was answered, as just four years later Hamish Small published the first paper on experimental HDC in the *Journal of Colloid and Interface Science* [17]. Using HDC columns packed with solid, impermeable spheres as part of the experimental set-up shown in Figure 3, Hamish was able to separate and determine the particle size of homo- and copolymeric latexes, of carbon black, to study the kinetics of particle growth during emulsion

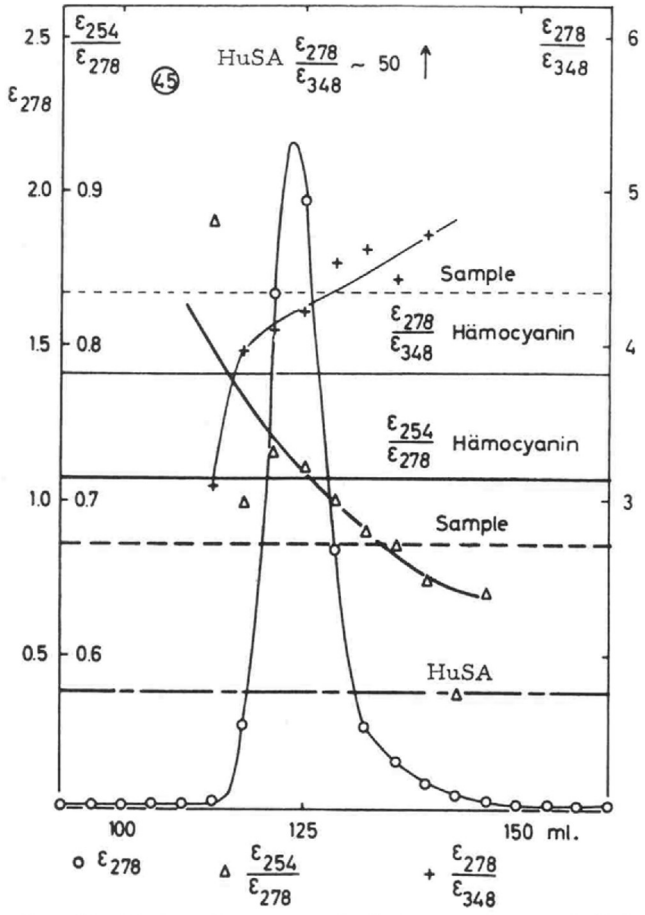

FIG. 10. Elution diagram obtained for a mixture of *Helix* hemocyanin and human serum albumin (Fig. 6A) on a column packed with glass spheres having diameters in the region 20–35 μ (see text).

Figure 2. Petersen demonstrated, in 1962, the separation of *Helix* hemocyanin and human serum albumin (HuSA) via a hydrodynamic chromatography mechanism operating in the interstitial column space. His explanation of the results lacked sufficient generality for it to apply to HDC separations in general. See [12] for details. (Reproduced from [12] with requested permission from Elsevier).

polymerization, and more, thus marking the advent of experimental HDC.

Many of the chromatographic underpinnings of HDC were developed in the late-1980s and throughout the 1990s, mostly in Europe and, therein, mostly in The Netherlands, by scientists such as Hans Poppe, Rob Tijssen, and others. Details of how their work impacted our understanding of retention, band broadening, and resolution in HDC are given in reference [8] and, thus, not discussed further here. We will discuss one particular example of work from Poppe's group, a 1991 publication in the

Hydrodynamic Chromatography
A Technique for Size Analysis of Colloidal Particles

HAMISH SMALL

Physical Research Laboratory, The Dow Chemical Company, Midland, Michigan 48640

Received November 14, 1973; accepted March 19, 1974

When colloidal materials are carried in aqueous suspension through packed beds of spherical particles, it has been observed that the rate of transport of the colloidal particles depends on such factors as the size of the colloid, the size of the packing and the ionic composition of the aqueous phase. From such observations, a chromatographic technique has been developed, called hydrodynamic chromatography, which can yield size information on a variety of colloidal materials in the submicron range. Several examples are provided that illustrate how the technique is applied in the study of polymer latexes to determine particle size, assess particle size distribution, follow emulsion polymerization kinetics and provide evidence for particle agglomeration. The origin of the various transport and separation phenomena is also discussed.

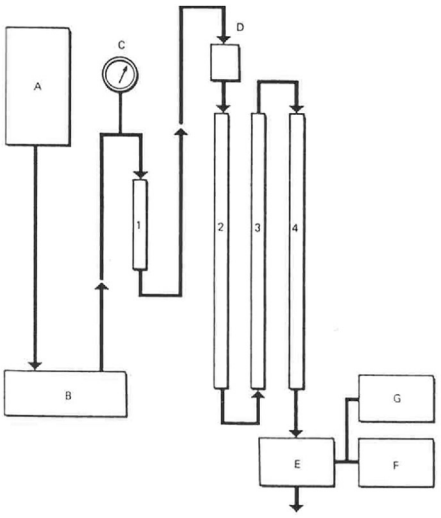

FIG. 1. Schematic diagram of HDC apparatus. A—reservoir; B—pump; C—pressure gauge; D—sample injection valve; E—detector; F—recorder; G—computer.

Figure 3. Hamish Small's original paper on experimental HDC in the *Journal of Colloid and Interface Science* in 1974, and apparatus employed therein. The HDC columns, 2 through 4 in the figure, were packed with solid, impermeable spheres. See [17] for details. (Reprinted from reference [17] with permission from Elsevier).

Journal of Chromatography in which the authors analyzed both toluene and a series of eight narrow-dispersity linear polystyrene (PS) standards ranging in molar mass M from 2.2×10^3 g mol^{-1} to 4×10^6 g mol^{-1}, in tetrahydrofuran at room temperature, using a size-exclusion chromatography column with an exclusion limit of 5×10^4 g mol^{-1} as determined by the manufacturer employing identical analytes and experimental conditions to those used by Poppe and colleagues [18]. It was observed that all analytes with an $M < 5 \times 10^4$ g mol^{-1} (analytes 6 through 9 in Figure 4) eluted in an order inversely proportional to their molar mass (which, for a series of linear polymers of the same monomeric composition, corresponds to an order inversely proportional to their size). The expectation would be for analytes 1 through 5, *i.e.,* those with $M > 5 \times 10^4$ g mol^{-1}, to elute together, as a single peak, at the exclusion volume of the SEC column. What is observed instead in Figure 4 is that analytes 1 through 5 are actually separated from each other. This occurred by means of an HDC mechanism operating in the interstitial medium of the SEC column. The reason this latter separation was able to occur is because the compounds being thus separated were so large, compared to the size of the pores in the column packing material, that the column packing particles appeared as impermeable to the analytes (one can think of these as "essentially" or "virtually" non-porous columns). These results opened the door for a wide variety of small-pore SEC columns to be employed for packed-column HDC. (It should be noted that the work by our group presented herein employed columns packed with actually, not virtually, impermeable particles).

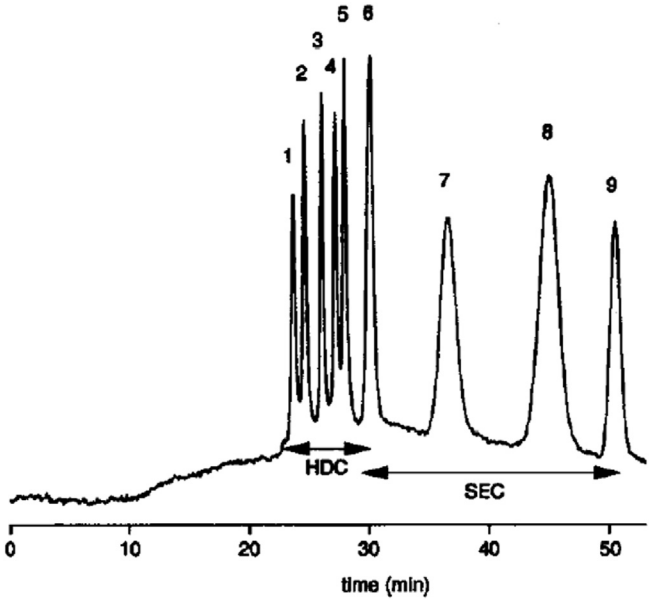

Figure 4. HDC separation within the interstitial medium of an SEC column with an exclusion limit of 5×10^4 g mol^{-1}, for analytes much larger than the packing particle pore size. Analytes 1 through 8 are narrow dispersity PS standards with molar mass, in g mol^{-1}, of (1) 4×10^6, (2) 2.2×10^6, (3) 7.5×10^5, (4) 3.36×10^5, (5) 1.27×10^5, (6) 4.39×10^4, (7) 1.25×10^4, (8) 2.2×10^3, analyte 9 is toluene. See [18] for details. (Reprinted from reference [18] with permission from Elsevier).

3. Packed-column, multi-detector HDC

For a well-packed column under laminar flow conditions, the interstitial medium can be considered a series of interconnected capillaries wherein a parabolic flow profile will develop [19], as shown in Figure 5 and akin to what was depicted in Figure 1 for the open tube scenario. The experiments from our lab detailed herein employ HDC columns packed with solid, non-porous particles with a diameter d_p of 20 μm. This large particle size is meant to maximize the interstitial distance between particles, a measure of which is provided by the hydraulic radius r_c of a column bed (Figure 5), and serves to minimize the interstitial shear rates $\dot{\gamma}$ to which analytes are exposed during their passage through the HDC columns, as per equation (1) [8, 20, 21, 22]:

$$\dot{\gamma} = \frac{4Q}{\varepsilon A r_c} \tag{1}$$

where Q is the volumetric flow rate through the column, ε the porosity of the packed bed, A the cross-sectional area of the column, and the hydraulic radius r_c is defined according to equation (2) as [20, 21, 22]:

$$r_c = \frac{d_p \varepsilon}{3(1-\varepsilon)} \tag{2}$$

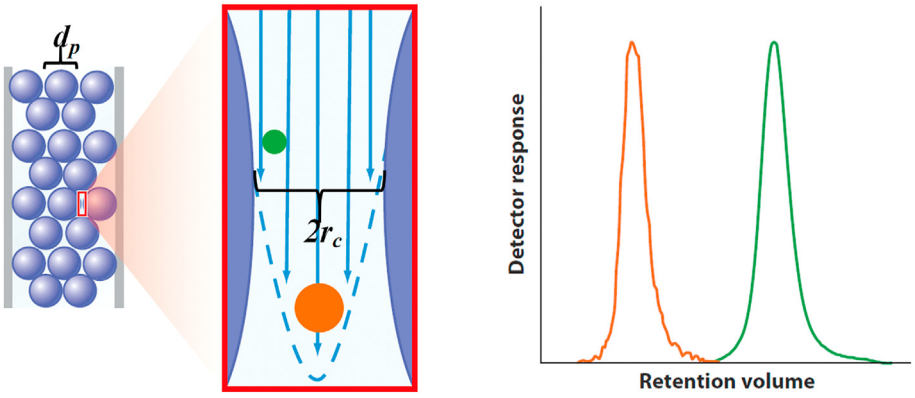

Figure 5. Separation in packed-column HDC. The interstitial medium can be considered a series of interconnected capillaries wherein, under laminar flow conditions, a parabolic flow profile develops. As in open tube case shown in Figure 1, larger analytes remain nearer the center of the interstitial medium, preferentially experiencing faster streamlines of flow and faster average velocities, as compared to their smaller-sized counterparts. Consequently, larger analytes elute from the HDC column ahead of smaller ones. Employing large d_p packing particles maximizes r_c, thus minimizing the interstitial shear rate $\dot{\gamma}$. (Adapted from [8]).

If, into these packed HDC columns we inject the large and small analytes depicted generically in Figure 1, the larger analyte will remain nearer the center of the interstitial medium and so will preferentially experience the faster streamlines of flow. The center of mass of the smaller analyte will be able to approach the walls of the column packing particles more closely than will the center of mass of the larger particle. Because of this, the smaller particle will be able to experience not only the faster streamlines near the center of the interstitial medium but also the slower streamlines near the particle walls. This results in the smaller particle traveling through the column with a slower average velocity, and eluting from the column later, than the larger particle, as depicted in Figure 5 and analogous to what occurs in the open tube scenario described at the outset of this section.

As mentioned earlier, Hamish Small's original publication on experimental HDC dates from 1974. Work in our lab on multi-detector HDC began in the mid-2000s, *i.e.,* about three decades later. While it would certainly be unfair to claim that there were no publications on HDC during that time, stating here that there was a paucity of applications publications would not likely meet with great resistance. (In addition to the fundamental papers alluded to in the Introduction, a small number of papers on dual-detector HDC can also be found in the literature [23, 24, 25, 26, 27]). This begs the question as to why there weren't more publication applying HDC during that 30-year period. Part of the answer to the question lies in the fact that packed-column HDC is a low chromatographic resolution technique, something which, for the most part, cannot be aided by multiple detectors. (Microcapillary HDC, which is beyond the topic of our present discussion, does provide for a large improvement in peak capacity, but at the expense of being limited to using a single detection method, generally laser induced fluorescence). A bigger issue, though, and one which also plagued flow field-flow fractionation until it was successfully and routinely coupled to on-line light scattering detection, is that HDC generally relied on calibration curves and flow markers to obtain particle size and its distribution. However, because the flow markers and calibrants oftentimes bore little, if any, chemical and/or physical resemblance to the analytes themselves, the results obtained were of questionable accuracy and, thus, of limited use. Furthermore, HDC analyses were almost always performed in single-detector mode, usually employing a UV/visible spectrophotometer operating in so-called "light obscuration" mode, which provided quite limited (usually no) information on particle shape or macromolecular structure.

The approach which we undertook in our lab consisted of coupling a multiplicity of physicochemical detectors, usually three or more, to an HDC separation. Depending of the type of detectors employed, a variety of advantages can be gained by this approach as compared to its single-detector counterpart. Before highlighting some of these advantages, let us speak briefly of the detectors involved in the study showcased in this paper.

4. On-line detection: refractometry, static and dynamic light scattering, viscometry

Because the fundamentals and hardware of the various detection methods employed have been described in extensive detail in a number of reviews and books (see e.g., references [11, 28, 29, 30, 31], only a cursory introduction is given here. Additionally, details about the experimental set-up and the particular hardware and conditions employed in the work discussed below can be found in reference [6].

4.1. Differential refractometry (DRI)

A DRI is a concentration-sensitive detector. Its response DRI_{resp} is proportional to the product of the concentration c of analyte in solution and the specific refractive index increment $\partial n/\partial c$ of the solution [32], as per equation (3):

$$DRI_{resp} \propto c \times \frac{\partial n}{\partial c} \tag{3}$$

It is necessary to measure the analyte concentration in each slice eluting from the HDC columns to provide quantitative meaning to much of the information (molar mass, sizes, etc.) from the other on-line detectors. The proportionalites in Eq. (3) and in Eqs. (4) and (5) below become equalities through the calibration constants for the particular pieces of hardware employed.

4.2. Multi-angle static light scattering (MALS)

A MALS detector measures the light scattered by a solution in excess of that scattered by the solvent, simultaneously at a series of angles θ, *i.e.,* it measures the excess Rayleigh factor $\Delta R(\theta)$ in Eq. (4a). The intensity of the scattered light provides a measure of analyte molar mass (namely, the weight-average molar mass M_w), while the angular dependence of the scattered light provides a measure of size (the z-average radius of gyration $R_{G,z}$). The cornerstone relationship of light scattering is the Rayleigh-Gans-Debye approximation, given by equations 4a-c:

$$\frac{\Delta R(\theta)}{K^* c} \propto M_w P(\theta)[1 - 2A_2 c M_w P(\theta)] \tag{4a}$$

where

$$K^* = \frac{4\pi^2 n_0^2 (\partial n/\partial c)^2}{\lambda_0^4 N_A} \tag{4b}$$

and

$$P(\theta) = 1 + \frac{16\pi^2}{\lambda^2} R_{G,z}^2 \sin^2\left(\frac{\theta}{2}\right) + \ldots \tag{4c}$$

Table 1. Three principal colloidal radii: Definition and methods of measurement.

Radius	Mathematical Definition	Conceptual Definition	HDC On-Line Measurement Method
Root-mean-square radius ("radius of gyration")	$R_G = \sqrt{\left(\frac{1}{n+1}\right)\sum_i (r_i - R_{cm})^2}$	Root-mean-square distance of any atom or group of atoms from molecule's or particle's center of mass	MALS + DRI
Hydrodynamic ("Stokes") radius	$R_H \equiv \frac{k_B T}{6\pi\eta_0 D}$	Radius of homogeneous hard sphere with identical D to analyte	DLS/QELS + DRI
Viscometric radius	$R_\eta \equiv \left\{\frac{3[\eta]M}{10\pi N_A}\right\}^{1/3}$	Radius of homogeneous hard sphere that changes viscosity of solution (compared to that of neat solvent) by same amount as analyte	SLS + VISC + DRI

A concentration-sensitive detector (*e.g.,* DRI) is needed to determine radius distribution and statistical moments thereof. MALS: Multi-angle static light scattering; DRI: Differential refractometry; DLS: Dynamic light scattering; QELS: Quasi-elastic light scattering; SLS: Static light scattering; VISC: Viscometry. n: number of atoms or groups; r_i: coordinate of particular atom or group; R_{CM}: coordinate of center of mass; k_B: Boltzmann's constant; T: absolute temperature; η_0: viscosity of solvent at experimental conditions; D: translational diffusion coefficient; $[\eta]$: intrinsic viscosity; M: molar mass; N_A: Avogadro's number.

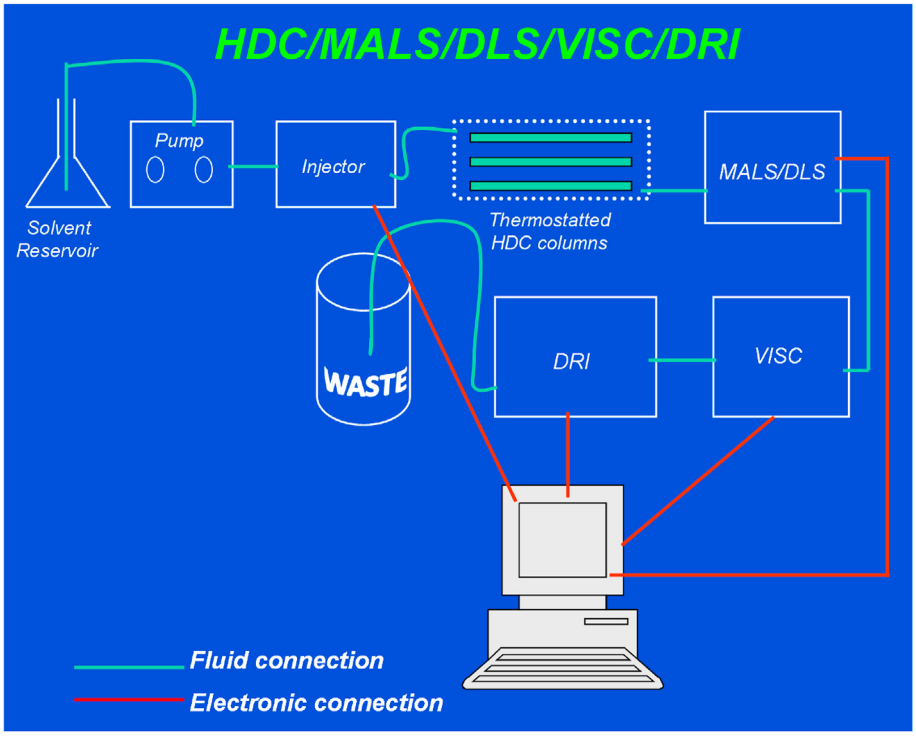

Figure 6. Schematic of the quadruple-detector (MALS/DLS/VISC/DRI) HDC set-up employed in the experiments described here.

In the above, A_2 is the second virial coefficient of the solution, n_0 the refractive index of the solvent at the experimental conditions, λ_0 is the vacuum wavelength of the incident radiation, N_A is Avogadro's number, $\lambda \equiv \lambda_0/n_0$ is the wavelength of the radiation in the medium, and $P(\theta)$ is the particle scattering factor.

4.3. Dynamic light scattering (also known as quasi-elastic light scattering)

This detector is contained within the same housing as the MALS, where one of the MALS photodiodes has been replaced by an avalanche photodiode to perform DLS measurements on-line. In DLS, the time-dependence of the scattered light is measured, wherefrom the translational diffusion coefficient D of the analyte in solution is derived. From this coefficient, one obtains the hydrodynamic or Stokes radius R_H of the analyte. This radius is defined conceptually and mathematically in Table 1.

4.4. Viscometry

The response of the viscometer $VISC_{resp}$ is directly proportional to the specific viscosity η_{sp} of the solution, as given by equation (5):

$$VISC_{resp} \propto \eta_{sp} \tag{5}$$

The intrinsic viscosity $[\eta]$ of the solution, employed inter alia in the calculation of the viscometric radius R_η (see Table 1), is obtained by rationing the responses of the viscometer and the refractometer at each HDC elution slice, after correction for interdetector delay if the detectors are connected in series, or after correction for split ratio if the connection is in parallel, as per equation (6) [33, 34]:

$$[\eta] \equiv \lim_{c\to 0} \frac{\eta_{sp}}{c} \propto \frac{VISC_{resp}}{DRI_{resp}} \tag{6}$$

As described in references [7, 8], the information from the above detectors can be combined to obtain the following parameters:

- The molar mass distribution (MMD) and associated statistical moments, using MALS + DRI.
- The distributions and associated statistical moments of the following size parameters:
  - o The radius of gyration (R_G), using MALS + DRI
  - o The hydrodynamic (Stokes) radius (R_H), using DLS/QELS + DRI
  - o The viscometric radius (R_η), using MALS + VISC + DRI

Table 2. Effect of flow rate on HDC results and comparison between on- and off-line MALS.

	M_n ($\times 10^7$ g mol^{-1})	M_w ($\times 10^7$ g mol^{-1})	M_z ($\times 10^7$ g mol^{-1})	Đ	$R_{G,z}$ (nm)	$R_{H,z}$ (nm)	$R_{\eta,w}$ (nm)
Off-line MALS	ND	1.44 +/- 0.08	ND	ND	50 +/- 1	ND	ND
4-detector HDC (0.5 mL min^{-1})	1.29 +/- 0.01	1.51 +/- 0.01	2.11 +/- 0.03	1.17 +/- 0.01	50 +/-1	28 +/- 1	24 +/- 1
4-detector HDC (1.0 mL min^{-1})	1.21 +/- 0.01	1.47 +/- 0.05	2.06 +/- 0.12	1.22 +/- 0.06	48 +/- 1	27 +/- 1	25 +/- 1

$Đ \equiv M_w/M_n$, ND: not determinable by off-line MALS. For on-line analyses, uncertainties correspond to one experimental standard deviation, based on $n \geq 4$; for off-line analysis, uncertainties correspond to instrumental standard deviation based on individual variances of all 16 MALS photodiodes. Subscripts *n*, *w*, and *z* denote, respectively, the number-, weight-, and *z*-averages of a particular property, be it molar mass or radius. All results obtained in aqueous eluent at room temperature; see [6] for experimental details.
Source: Ref. [6].

- Shape and compactness of the sample, through the dimensionless parameter $\rho \equiv R_{G,z}/R_{H,z}$, obtained using MALS + QELS.
- Structure and compactness of the sample, through the dimensionless ratio $R_{\eta,w}/R_{G,z}$, obtained using MALS + VISC + DRI.

To determine the size parameters in Table 1, along with a host of other properties, we employ the system shown schematically in Figure 6. This is immediately recognizable for its resemblance to a typical liquid chromatographic instrumental set-up, containing such standard components as an inlet reservoir (for solvent, in the case of macromolecules, or for carrier medium, in the case of colloids), pump, injector, etc. The columns, which should be kept in a thermostatted compartment if dimensions permit are, as was mentioned above, packed with large particle diameter, impermeable (*i.e.,* non-porous) particles to minimize the on-column interstitial shear rates to which analytes are subjected. After the columns comes the "heart" of any multi-detector system, namely, the detectors. In our case and, specifically, for the experiments described below, we employed a quadruple-detector system consisting of a multi-angle static light scattering (MALS) detector which measures the scattered light at 16 different angles simultaneously; in the same housing as the MALS is a dynamic light scattering (a.k.a. quasi-elastic light scattering) detector with variable-angle capability (though most DLS measurements were conducted at a single, fixed angle); this is followed by a differential viscometer (VISC); and, at the end of the detector train, there is a differential refractometer (DRI), a concentration-sensitive detector because, as mentioned earlier, to quantitate much of the information resultant from measurements employing MALS, DLS, and VISC, one must measure the analyte concentration in each slice eluting from the HDC columns.

5. An object lesson: quadruple-detector HDC analysis of elongated colloidal silica [6]

We describe here the HDC/MALS/DLS/VISC/DRI analysis of a commercially available colloidal silica dispersion [6]. Real-world applications of this type of material include as a coating for paper, plastics, and metals; as a binder for ceramics, glass, and fibers; and as a modifier for paints and coatings. Transmission electron microscopy (TEM) data from the manufacturer (confirmed by in-house TEM measurements) indicated that the silica particles in this particular colloidal dispersion possess an elongated structure, with lengths of 40 nm–100 nm and widths between 9 nm to 15 nm.

Generally, the first thing we do in our lab before performing any on-line analyses is to perform off-line MALS analysis of the sample. This is done by injecting the analyte solution or suspension (the latter, in the present case) directly into the MALS cell, after having decoupled this detector from the HDC columns. Off-line MALS experiments allow determination of whether or not the analyte has degraded during its passage through the HDC columns by comparing the weight-average molar mass (M_w) and *z*-average radius of gyration ($R_{G,z}$) obtained by off-line MALS to those measured when the detector is connected on-line to the HDC columns.

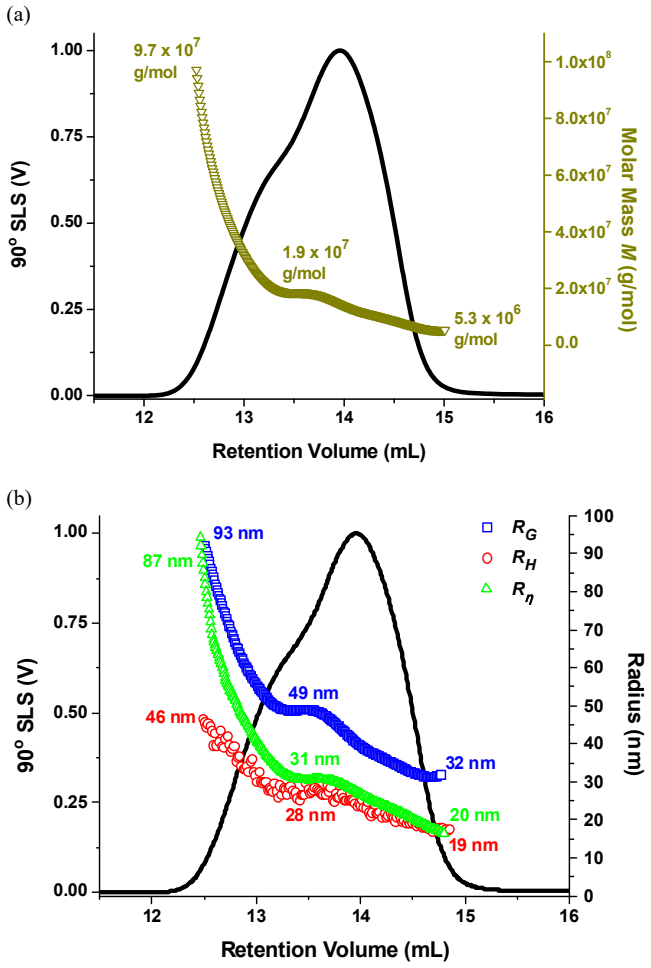

Figure 7. HDC/MALS/DLS/VISC/DRI analysis of elongated colloidal silica. (a) Molar mass as a function of retention volume. (b) Size (R_G, blue open squares; R_H, red open circles, and R_η, green open triangles) as a function of retention volume. In both figures, chromatogram (black solid line, tied to left ordinate) is that determined by 90° MALS photodiode. See [6] for details. (Reproduced from reference [6] with permission from The Royal Society of Chemistry).

Results from off-line MALS experiments for the colloidal silica sample are shown in Table 2, where they are contrasted with those obtained by on-line MALS at two different flow rates. The agreement between these sets of values is a good indication that no measurable analyte degradation has occurred in the HDC columns.

As seen in Table 2, the HDC experiments were conducted at two different flow rates, differing from one another by a factor of two. Results for the various molar mass averages and molar mass dispersity, as well as for all averages of the three radii measured (only one statistical average of each radius is given in Table 2; for a more complete set of results, see

Table 3. Determining particle shape from combined MALS and DLS results.

$\rho \equiv R_{G,z}/R_{H,z}$	Structure
0.778	Hard sphere
0.875 to 0.987	Oblate ellipsoid
1.36 to 2.24	Prolate ellipsoid
2.36	Rigid rod

Sources: Refs. [6, 35, 36, 37, 38, 39, 40].

ref. [6]), show no significant change as a function of flow rate. This agreement between data sets provides, if not absolute, then certainly strong circumstantial evidence that the colloidal silica is eluting via a near-ideal HDC mechanism, *i.e.,* in the absence of any measurable enthalpic contributions to the separation, as retention in ideal HDC is due solely to the solution translational entropy ΔS^{trans} of analytes (see ref. [8] for a more detailed discussion).

The chromatogram in Figure 7a,b is that obtained by the 90° photodiode of the MALS detector. As seen in Figure 7a, the molar mass of the sample ranges from $\approx 5 \times 10^6$ g mol^{-1} to $\approx 1 \times 10^8$ g mol^{-1}, while Figure 7b shows that its size ranges from ≈20 nm to just over 90 nm. Additionally, extensive work has been done by various groups showing how the *z*-averages of R_G and R_H can combine into a dimensionless parameter given the symbol ρ, theoretical values for which have been calculated for a variety of structures. Some of the values, apposite to the present discussion, are given in Table 3. For the ellipsoids, the range of values represents the fact that an exact value depends on the axial ratio of a particular ellipse, *i.e.,* on the ratio of semi-major to semi-minor axes. Given that the present experiments employ both MALS and DLS as on-line detection methods, this affords determination of ρ for each common HDC chromatographic slice. Traditionally, one would represent the structural information thus gained as a plot of ρ as a function of retention volume, overlaid upon a chromatogram of the sample. Here, we have opted to use the values of ρ given in Table 3 to show, in Figure 8, the R_G versus R_H relationships for the different structures across a broad range of both radii. What is gleaned from Figure 8, where the ρ values for the sample, based on the experimentally-determined R_G and R_H, are shown as filled magenta squares, is that across its size distribution the colloidal silica retains a prolate ellipsoidal structure. This is an example of true detector synergism, as combining the size information obtained by both MALS and DLS afford structural information not produced by either detector.

As described above and shown in Table 1, a third size parameter additional to R_G and R_H is the viscometric radius R_η, determined by combining the molar mass information from MALS with the intrinsic viscosity [η] information from on-line viscometry (VISC) detection (in both the case of MALS and VISC, the concentration information from the DRI is needed as well for this). The weight-average viscometric radius $R_{\eta,w}$ has been combined with $R_{G,z}$ in the form of another dimensionless size parameter akin to ρ (but for which a symbol name has not been assigned), also informative of macromolecular and colloidal structure [11]. While not as many values of R_η/R_G have been derived in the literature as have been for ρ, it is known that $R_\eta/R_G = (5/3)^{0.5}$ (≈1.3) for a homogeneous hard sphere [41, 42] and $R_\eta/R_G \approx 0.3$ to 0.4 for rigid rods [43], with random coil homopolymers adopting values somewhere in between these two extremes depending on branching, degree of rigidity, and dilute solution thermodynamics [11, 42, 44, 45, 46]. (The subscripts denoting the particular statistical moment of each radius have been dropped, both for simplicity and because of the relatively narrow dispersity of the HDC elution slices) For the purposes of the present discussion, it is important to realize that a larger value of R_η/R_G corresponds to analytes adopting a more compact structure in solution, whereas smaller values of this radii ratio correspond to analytes adopting a more extended structure.

Figure 9 shows a plot of R_η/R_G as a function of retention volume. As a guide, both the hard sphere limit and the rigid rod region have been placed on the plot. What is observed for the colloidal silica is that, as retention volume increases, R_η/R_G decreases, from 0.94 at early elution volumes to 0.63 at later ones. This signifies that, as elution volume increases, the sample adopts a more extended conformation in solution.

Tying together the results from the quadruple-detector HDC analysis employing on-line MALS, DLS, VISC, and DRI, we first observe that, as retention volume increases the size of the colloidal silica decreases, in accordance with our earlier explanation of the HDC retention mechanism by which larger analytes were predicted to elute ahead of smaller ones. As size decreases, so does molar mass; bigger colloids have larger mass than do smaller ones. Throughout these changes in size and molar mass, the sample retains a prolate ellipsoidal conformation. However, as the prolate ellipsoids become smaller they also become more extended. This does not mean that the ellipsoids are becoming larger; rather, that the axial ratio is shifting in favor of the semi-major axis of the ellipses. As can be seen in Figure 10, the mutual interdependence of size, molar mass,

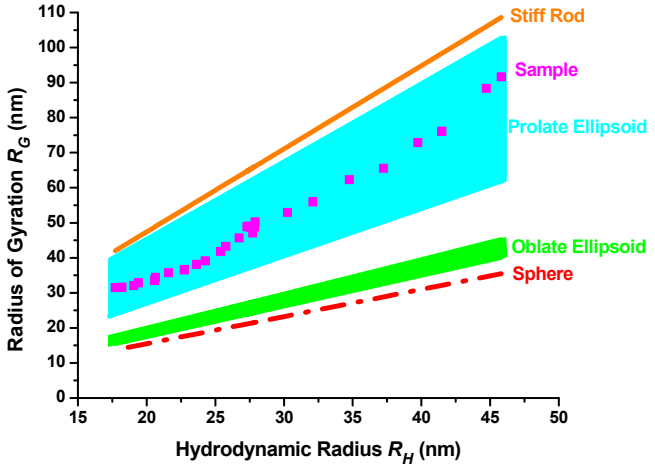

Figure 8. Relationship between radius of gyration and hydrodynamic radius, as given by theoretical calculations of dimensionless parameter ρ for various structures. Overlaid upon these, in filled magenta squares, are R_G versus R_H relationships for the colloidal silica sample across its size range, based on MALS and DLS on-line with HDC separation. See [6] for details. (Reproduced from reference [6] with permission from The Royal Society of Chemistry).

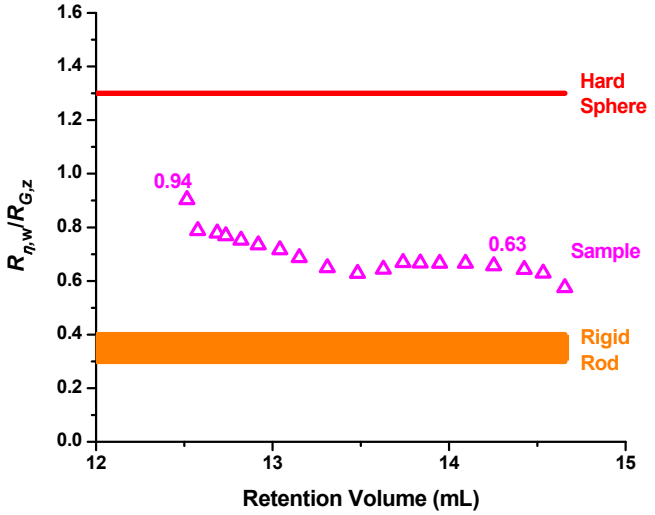

Figure 9. Change in dimensionless radii ratio R_η/R_G as a function of HDC retention volume. Hard sphere limit (solid red line) and rigid rod region (orange section) are given as guides. Ratios based on experimentally determined data from on-line MALS and VISC are shown as open magenta triangles. See [6] for details. (Reproduced from reference [6] with permission from The Royal Society of Chemistry).

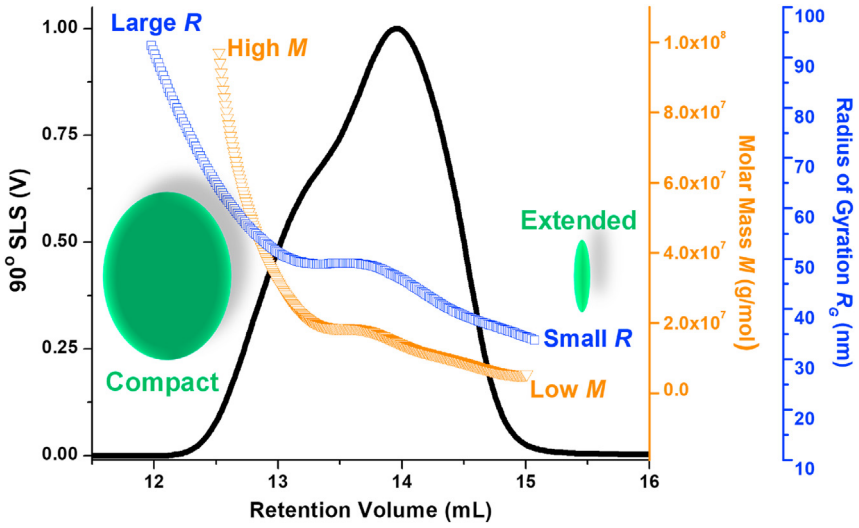

Figure 10. Interrelationships of colloidal silica size, molar mass, shape, and structure, continuously across the chromatogram, as determined by HDC/MALS/DLS/VISC/DRI. See [6] for details.

shape, and structure can be determined, all as a function of one another, continuously across the chromatogram by employing HDC as a separation tool and coupling it on-line to MALS, DLS, VISC, and DRI detection.

6. Conclusions

Demonstrated here is how coupling a multiplicity of detectors to a hydrodynamic chromatography separation affords a very powerful technique for studying polymers, particles, and colloids. With it, one can determine size, molar mass, shape, structure, and their distributions, as well as their interdependences, continuously across a chromatogram.

Packed-column HDC remains a low-resolution chromatographic technique. This can be compensated for, to a certain (very limited) extent, by the use of multiple detectors [2]. A more powerful incarnation of HDC, as regards resolution, is microcapillary HDC, where dozens of peaks can be separated during the course of one experiment [47, 48]. The choice of detectors in the latter case, however, is limited (usually laser-induced fluorescence is employed) and, thus, so is the information obtainable about the analytes.

HDC has become an attractive method for samples that cannot be analyzed by size-exclusion chromatography [3, 4, 49], either because they degrade during their passage through the SEC columns or because the extremely low flow rates that would be required to avoid this degradation result in impracticably long analysis times. And, while HDC is not going to replace or displace flow field-flow fractionation as an analytical method, the former can be a cost-effective alternative to the latter and perhaps something to be considered before effecting a major capital outlay. If a multi-detector SEC system is already in place in a laboratory, all that is needed is to replace the SEC columns with HDC columns, and to apply a bit of chromatographic and polymer or colloid science ingenuity to the design of experiments and interpretation of data.

Declarations

Author contribution statement

All authors listed have significantly contributed to the development and the writing of this article.

Funding statement

This research did not receive any specific grant from funding agencies in the public, commercial, or not-for-profit sectors.

Data availability statement

No data was used for the research described in the article.

Declaration of interests statement

The authors declare no conflict of interest.

Additional information

No additional information is available for this paper.

Acknowledgements

The author would like to thank Drs. Samantha L. Isenberg (Centers for Disease Control and Prevention), Leena Pitkänen (Aalto University) and, especially Amandaa K. Brewer (Arkema) for their work with the author on various aspects of HDC over the years, during our time together first at Florida State University and then at NIST. Commercial products are identified to specify adequately the experimental procedure. Such identification does not imply endorsement or recommendation by the National Institute of Standards and Technology, nor does it imply that the materials identified are necessarily the best available for the purpose.

References

[1] A.K. Brewer, A.M. Striegel, Particle size characterization by quadruple-detector hydrodynamic chromatography, Anal. Bioanal. Chem. 393 (2009) 295–302.
[2] A.K. Brewer, A.M. Striegel, Hydrodynamic chromatography of latex blends, J. Separ. Sci. 33 (2010) 3555–3563.
[3] S.L. Isenberg, A.K. Brewer, G.L. Côté, Hydrodynamic versus size-exclusion chromatography characterization of alternan, and comparison to off-line MALS, Biomacromolecules 11 (2010) 2505–2511.
[4] A.K. Brewer, A.M. Striegel, Characterizing string-of-pearls colloidal silica by multidetector hydrodynamic chromatography and comparison to multidetector size-exclusion chromatography, off-line multiangle static light scattering, and transmission electron microscopy, Anal. Chem. 83 (2011) 3068–3075.
[5] A.K. Brewer, A.M. Striegel, Characterizing a spheroidal nanocage drug-delivery vesicle using multi-detector hydrodynamic chromatography, Anal. Bioanal. Chem. 399 (2011) 1507–1514.
[6] A.K. Brewer, A.M. Striegel, Characterizing the size, shape, and compactness of a polydisperse prolate ellipsoidal particle *via* quadruple-detector hydrodynamic chromatography, Analyst 136 (2011) 515–519.
[7] A.M. Striegel, Hydrodynamic chromatography: Packed columns, multiple detectors, and microcapillaries, Anal. Bioanal. Chem. 402 (2012) 77–81.
[8] A.M. Striegel, A.K. Brewer, Hydrodynamic chromatography, Annu. Rev. Anal. Chem. 5 (2012) 15–34.
[9] A.M. Striegel, Hamish Small: Experimenter extraordinaire, LC-GC Eur. 28 (11) (2015) 606–611.

[10] A.M. Striegel, Hamish Small: Experimenter extraordinaire, LC-GC N. Am. 33 (10) (2015) 776–781.
[11] A.M. Striegel, W.W. Yau, J.J. Kirkland, D.D. Bly, Modern Size-Exclusion Liquid Chromatography, second ed., Wiley, Hoboken, NJ, 1999.
[12] K.O. Pedersen, Exclusion chromatography, Arch. Biochem. Biophys. Suppl. 1 (1962) 157–168.
[13] E.A. DiMarzio, C.M. Guttman, Separation by flow, Polym. Lett. 7 (1969) 267–272.
[14] E.A. DiMarzio, C.M. Guttman, Separation by flow, Macromolecules 3 (1970) 131–146.
[15] E.A. DiMarzio, C.M. Guttman, Separation by flow. II. Application to gel permeation chromatography, Macromolecules 3 (1970) 681–691.
[16] E.A. DiMarzio, C.M. Guttman, Separation by flow and its application to gel permeation chromatography, J. Chromatogr. 55 (1971) 83–97.
[17] H. Small, Hydrodynamic chromatography. A technique for size analysis of colloidal particles, J. Colloid Interface Sci. 48 (1974) 147–161.
[18] G. Stegeman, J.C. Kraak, H. Poppe, Hydrodynamic and size-exclusion chromatography of polymers on porous particles, J. Chromatogr. 550 (1991) 721–739.
[19] J.C. Giddings, Dynamics of Chromatography, Marcel Dekker, New York, 1965.
[20] A.M. Striegel, Observations regarding on-column, flow-induced degradation during SEC analysis, J. Liq. Chromatogr. Relat. Technol. 31 (2008) 3105–3114.
[21] A.M. Striegel, S.L. Isenberg, G.L. Côté, An SEC/MALS study of alternan degradation during size-exclusion chromatographic analysis, Anal. Bioanal. Chem. 394 (2009) 1887–1893.
[22] A.M. Striegel, Do column frits contribute to the on-column, flow-induced degradation of macromolecules? J. Chromatogr. A 1359 (2014) 147–155.
[23] M.A. Langhorst, F.W. Stanley Jr., S.S. Cutié, J.H. Sugarman, L.R. Wilson, D.A. Hoagland, R.K. Prud'homme, Determination of nonionic and partially hydrolyzed polyacrylamide molecular weight distributions using hydrodynamic chromatography, Anal. Chem. 58 (1986) 2242–2247.
[24] G. von Wald, M. Langhorst, Particle size distribution II: assessment and characterization, in: T. Proved (Ed.), ACS Symp. Ser. 472, American Chemical Society, Washington, DC, 1991, pp. 308–323.
[25] J.A. Klavons, F.R. Dintzis, M.M. Millard, Hydrodynamic chromatography of waxy maize starch, Cereal Chem. 74 (1997) 832–836.
[26] Y. Liu, W. Radke, H. Pasch, Coil-stretch transition of high molar mass polymers in packed-column hydrodynamic chromatography, Macromolecules 38 (2005) 7476–7484.
[27] Y. Liu, W. Radke, H. Pasch, Onset of the chromatographic mode transition from hydrodynamic chromatography to slalom chromatography: an effect of polymer stretching, Macromolecules 39 (2006) 2004–2006.
[28] Multiple detection in size-exclusion chromatography, in: A.M. Striegel (Ed.), ACS Symp. Ser. 893, American Chemical Society, Washington, DC, 2005.
[29] A.M. Striegel, Size-exclusion chromatography, in: S. Fanali, P.R. Haddad, C.F. Poole, M.-L. Riekkola (Eds.), Liquid Chromatography: Fundamentals and Instrumentation, second ed., Elsevier, Amsterdam, 2017, pp. 245–273.
[30] A.M. Striegel, Multiple detection in size-exclusion chromatography of macromolecules, Anal. Chem. 77 (2005) 104A–113A.
[31] P.J. Wyatt, Light scattering and the absolute characterization of macromolecules, Anal. Chim. Acta 272 (1993) 1–40.
[32] A.M. Striegel, Specific refractive index increment ($\partial n/\partial c$) of polymers at 660 nm and 690 nm, Chromatographia 80 (2017) 989–996.
[33] A.M. Striegel, Viscometric detection in size-exclusion chromatography: Principles and select applications, Chromatographia 79 (2016) 945–960.
[34] A.M. Striegel, S.P. Trainoff, Entropic-based separation of diastereomers. Size-exclusion chromatography with on-line viscometry and refractometry detection for analysis of blends of mannose and galactose methyl-α-pyranosides at "ideal" size-exclusion conditions, Chromatographia 84 (2021) 37–45.
[35] W. Burchard, Solution properties of branched macromolecules, Adv. Polym. Sci. 143 (1999) 113–194.
[36] M. Antoniette, S. Heinz, M. Schmidt, C. Rosenauer, Determination of the micelle architecture of polystyrene/poly (4-vinylpyridine) block copolymers in dilute solution, Macromolecules 27 (1994) 3276–3281.
[37] K. Matsuoka, A. Yonekawa, M. Ishii, C. Honda, K. Endo, Y. Moroi, Y. Abe, T. Tamura, Micellar size, shape and counterion binding of N-(1,1-Dihydroperfluoroalkyl)-N,N,N-trimethylammonium chloride in aqueous solutions, Colloid Polym. Sci. 285 (2006) 323–330.
[38] W. Van De Sande, A. Persoons, The size and shape of macromolecular structures: determination of the radius, the length and the persistance length of rod-like micelles of dodecyldimethylammonium chloride and bromide, J. Phys. Chem. 89 (1985) 404–409.
[39] H. Slayter, J. Loscalzo, P. Bockenstedt, R.I. Handin, Native conformation of human von Willebrand protein. Analysis by electron microscopy and quasi-elastic light scattering, J. Biol. Chem. 260 (1985) 8559–8563.
[40] J. Loscalzo, H. Slayter, R.I. Handin, D. Farber, Subunit structure and assembly of von Willebrand factor polymer: complementary analysis by electron microscopy and quasielastic light scattering, Biophys. J. 49 (1986) 49–50.
[41] J. Roovers, Star and Hyperbranched Polymers, in: M.K. Mishra, S. Kobayashi (Eds.), Marcel Dekker, New York, 1999, pp. 285–341.
[42] A.M. Striegel, Influence of chain architecture on the mechanochemical degradation of macromolecules, J. Biochem. Biophys. Methods 56 (2003) 117–139.
[43] S.G. Ostlund, A.M. Striegel, Ultrasonic degradation of poly(g-benzyl-L-glutamate), an archetypal highly extended polymer, Polym. Degrad. Stabil. 93 (2008) 1510–1514.
[44] A.M. Striegel, Influence of anomeric configuration on mechanochemical degradation of polysaccharides: Cellulose versus amylose, Biomacromolecules 8 (2007) 3944–3949.
[45] I.A. Haidar Ahmad, D.A. Striegel, A.M. Striegel, How does sequence length heterogeneity affect the dilute solution conformation of copolymers? Polymer 52 (2011) 1268–1277.
[46] M.J. Morris, A.M. Striegel, The effect of styrene-methyl methacrylate monomeric arrangement on the ultrasonic degradation of copolymers, Polym. Degrad. Stabil. 97 (2012) 2185–2194.
[47] X. Wang, V. Veerappan, C. Cheng, X. Jiang, R.D. Allen, P.K. Dasgupta, S. Liu, Free solution hydrodynamic separation of DNA from 75 to 106 000 base pairs in a single run, J. Am. Chem. Soc. 132 (2010) 40–41.
[48] K.J. Liu, T.D. Rane, Y. Zhang, T.-H. Wang, Single-molecule analysis enables free solution hydrodynamic separation using yoctomole levels of DNA, J. Am. Chem. Soc. 133 (2011) 6898–6901.
[49] L. Pitkänen, A.R. Montoro Bustos, K.E. Murphy, M.R. Winchester, A.M. Striegel, Quantitative characterization of gold nanoparticles by size-exclusion and hydrodynamic chromatography, coupled to inductively coupled plasma mass spectrometry and quasi-elastic light scattering, J. Chromatogr. A 1511 (2017) 59–67.